Journal of Glaciology, Vol. 6, No. 48, 1967

THE EFFECT OF ABSORBED SOLAR RADIATION ON THE THERMAL DIFFUSION IN ANTARCTIC FRESH-WATER ICE AND SEA ICE

By G. Weller*

(Meteorology Department, University of Melbourne, Parkville, Victoria, Australia)

Abstract. Ice temperatures were measured on the ice plateau at Mawson, Antarctica, for one year down to depths of 11 m. and through a floating sea-ice cover for six months. The plateau data were examined by harmonic analysis and the thermal diffusivity of the ice was obtained from the classical model of heat diffusion. An improved model of heat diffusion proposed by Lettau (1954) was also used to derive the diffusivity. The results show that absorbed radiation affects the computed diffusivity values down to 6–8 m. depth and a model is put forward to explain these apparent changes with depth. Data on the extinction of radiation in the ice have been published elsewhere (Weller and Schwerdtfeger, in press). The diffusivity of the ice is determined for periods with no radiation in winter and the value of 0·011 cm.^{2} sec.$^{-1}$ agrees well with values at 8 m. depth where the effect of radiation becomes negligible.

Heat-flux plates embedded in the ice were used to determine the diffusivity independently and also to give numerical values of the heat flux at any moment. The geometry and characteristics of these flux plates are discussed elsewhere (Schwerdtfeger and Weller, 1967). They are also used to derive the diffusivity of sea ice and enable a detailed analysis of the diurnal heat flux in such complex substances as sea ice to be made.

Résumé. *L'effet de la radiation solaire absorbée sur la diffusion thermique de la glace d'eau douce et de mer dans l'Antarctique.* Les températures de la glace ont été mesurées sur le plateau de glace à la Station Mawson, Antarctique, pendant une année jusqu'à une profondeur de 11 m et à travers une couverture de glace de mer flottante pendant six mois. Les données obtenues sur le plateau ont été examinées par analyse harmonique et la diffusivité obtenue par le modèle classique de diffusion thermique. Un nouveau modèle de diffusion thermique proposé par Lettau (1954) a aussi été utilisé pour en déduire la diffusivité. Les résultats montrent que la radiation absorbée affecte la diffusivité jusqu'à une profondeur de 6 à 8 m. Il est proposé un modèle pour expliquer ces changements avec la profondeur. Les données sur l'extinction de la radiation dans la glace ont été publiées autre part (Weller et Schwerdtfeger, in press). La diffusivité de la glace a été déterminée dans les conditions de non radiation en hiver et la valeur de 0,011 cm^2 s^{-1} s'accorde bien avec les valeurs à 8 m de profondeur où l'effet de radiation devient négligeable.

Des plaques placées dans la glace pour la mesure du flux de chaleur ont aussi été utilisées pour en déduire indépendamment la diffusivité et aussi pour obtenir les valeurs du flux de chaleur à chaque moment. La géométrie et les caractéristiques de ces plaques ont été discutées autre part (Schwerdtfeger et Weller, 1967). Elles ont aussi été utilisées pour obtenir la diffusivité de la glace de mer et elles ont permis une analyse détaillée du flux de chaleur diurne.

Zusammenfassung. *Der Einfluss absorbierter Sonnenstrahlung auf die thermische Diffusion von antarktischem Süsswasser- und Meereis.* Eistemperaturen wurden ein Jahr lang auf dem Eisplateau bei Mawson, Antarktika, bis zu einer Tiefe von 11 m und über 6 Monate durch eine schwimmende Meereisdecke gemessen. Die Plateauwerte wurden harmonisch analysiert; ihre Durchlässigkeit wurde nach dem klassischen Modell der Wärmediffusion bestimmt. Daneben wurde ein verbessertes Modell der Wärmediffusion nach Lettau (1954) zur Ableitung der Durchlässigkeit benutzt. Die Ergebnisse zeigten, dass absorbierte Strahlung die Durchlässigkeitswerte bis zu 6–8 m Tiefe beeinflusst. Zur Erklärung dieser Tiefenabhängigkeit wird ein Modell entwickelt. Beobachtungen zur Strahlungsextinktion in Eis wurden anderwärts veröffentlicht (Weller und Schwerdtfeger, in press). Die Durchlässigkeit des Eises wurde für strahlungslose Verhältnisse im Winter bestimmt und der Wert von 0,011 cm^2 s^{-1} stimmt gut mit Werten in 8 m Tiefe überein, wo der Strahlungseinfluss vernachlässigbar wird.

Ins Eis eingelassene Wärmeleitplatten wurden zur unabhängigen Bestimmung der Durchlässigkeit und zur Ermittlung von Zahlenwerten des Wärmeflusses in jedem Zeitpunkt benutzt. Die Gestalt und die Kennwerte dieser Wärmeleitplatten wurden anderwärts erläutert (Schwerdtfeger und Weller, 1967). Sie wurden auch zur Bestimmung der Durchlässigkeit von Meereis herangezogen und ermöglichten eine Analyse des täglichen Wärmeflusses in so komplexen Substanzen wie Merreis.

Symbols

t = time, sec.,

z = depth below the surface, cm.,

T = temperature, °C.,

* Antarctic Division, Department of External Affairs, Australia, attached to the Meteorology Department, University of Melbourne.

B = vertical heat flux conducted in the z direction, cal. cm.$^{-2}$ sec.$^{-1}$,
k = heat conductivity at depth z, cal. cm.$^{-1}$ sec.$^{-1}$ deg.$^{-1}$,
C = heat capacity per unit volume at depth z, cal. cm.$^{-3}$ deg.$^{-1}$,
c = heat capacity per unit mass at depth z, cal. g.$^{-1}$ deg.$^{-1}$,
$K = k/C$ = thermal diffusivity at depth z, cm.^{2} sec.$^{-1}$,
Q = heat flux at depth z, cal. cm.$^{-2}$,
$\nu = \omega/2\pi$ = frequency of temperature or heat flux waves, sec.$^{-1}$,
A, a_n, b_n = amplitudes,
ϵ, α_n, β_n, γ_n = phase angles,
n = order of harmonic,
the prime ($'$) denotes partial differential with respect to z,
($\dot{}$) denotes partial differentiation with respect to t.

1. Introduction

Problems of the conduction of heat in solids with periodic surface temperature are of great practical importance. One of these is the study of the fluctuations in temperature of the surface layer of the Earth due to the periodic heating by the sun. In the following study this periodicity due to solar heating will be examined in three types of ice bodies: (a) homogeneous ice of semi-infinite thickness, (b) inhomogeneous ice of semi-infinite thickness, and (c) inhomogeneous ice of finite thickness.

If the surface temperature in the semi-infinite homogeneous solid at $z > 0$ is given by

$$T = A\cos(\omega t - \epsilon) \tag{1.1}$$

and the initial temperature is zero, then the temperature at depth z is given by the Fourier solution (Carslaw and Jaeger, 1959) as

$$T = A\exp[-z(\omega/2K)^{\frac{1}{2}}]\cos[\omega t - z(\omega/2K)^{\frac{1}{2}} - \epsilon]. \tag{1.2}$$

The amplitude of the temperature oscillation decreases as

$$\exp[-z(\omega/2K)^{\frac{1}{2}}] \tag{1.3}$$

and thus falls off more rapidly for large ω. Also there is a progressive lag

$$z(\omega/2K)^{\frac{1}{2}} \tag{1.4}$$

in the phase of the temperature wave. This lag increases with ω.

A measurement of either the amplitude or phase at depth z is thus sufficient to determine the diffusivity K. A third method of determining the diffusivity is applicable when the vertical flux of heat B is considered at the surface,

$$B = -k\left(\frac{\partial T}{\partial z}\right)_{z=0} = \left(\frac{\omega}{K}\right)^{\frac{1}{2}} kA\cos\left(\omega t - \epsilon + \frac{\pi}{4}\right) \tag{1.5}$$

and the amplitudes of temperature and heat flux fluctuations are known.

In the inhomogeneous case of heat conduction, i.e. when the heat conductivity and capacity of the medium are functions of depth, the above solutions are no longer applicable. Lettau (1954) has derived an exact solution of this case, where the thermal diffusivity is obtained on the basis of Fourier coefficients of the periodic fluctuations of temperature and heat flux at various depths. The procedure is described and applied in section 4 of this paper.

The last case of interest is that of a solid bounded by two parallel planes. A slab $0 \leqslant z \leqslant l$ is considered which has zero initial temperature and has the planes $z = 0$ and $z = l$ kept at temperatures zero and $\sin(\omega t + \epsilon)$ respectively. A Fourier solution of the diffusion equation exists for these boundary conditions and the amplitudes and phases are given by expressions which are discussed and applied to sea ice in section 11.

All these solutions apply strictly only to conditions of pure heat conduction resulting from temperature changes at the boundaries and are not applicable when other forms of energy transfer take place in the bodies considered. In transparent media such as ice and snow, the above conditions are however not fulfilled since large amounts of energy may be transferred into the medium by radiation. In the following study the effects of absorbed radiation on the thermal diffusion in fresh-water ice and sea ice will be investigated. The radiation extinction coefficients of these two types of ice were 0·007 cm.$^{-1}$ and 0·011 cm.$^{-1}$ respectively (Weller and Schwerdtfeger, in press).

2. Temperature Patterns in the Plateau Ice—Descriptive Analysis

Ice temperatures were measured on the coastal ice slopes near Mawson at 150 m. altitude during 1965. Copper-constantan thermocouples shielded with chromium plated copper tubes 6 mm. in diameter and *c.* 20 mm. long were used. The thermocouples were sealed in a length of polyethylene tubing and installed in a bore hole which was refilled with a snow–water mixture. The reference junction was immersed in a well insulated ice–water bath which was frequently renewed, and recording was by means of a multirange 12-channel Siemens potentiometric recorder which was housed in a heated caravan. Power to drive the recorder was provided by a wind generator, and periods of calms when no recording was made require a certain amount of interpolation of the data.

The daily midnight temperatures observed in the plateau ice at 1, 2, 4 and 8 m. depth are shown in Figure 1. On 1 December the temperature readings were discontinued and started at a new site approximately 100 m. lower on the plateau. The temperature difference at 8 m. depth can be seen to be 1 deg. which corresponds to the dry adiabatic lapse rate. All subsequent temperature measurements at all levels were corrected to the initial temperature set by subtracting 1 deg.

Half-monthly running means are shown in Figure 2. The 11 m. temperatures were largely extrapolated from readings in December, January and February at the new site. Temperature isopleths in a depth–time coordinate system are shown in Figure 3. The penetration of the annual temperature wave is clearly shown in this diagram. Finally tautochrones showing temperature vs. depth for monthly intervals are shown in Figure 4.

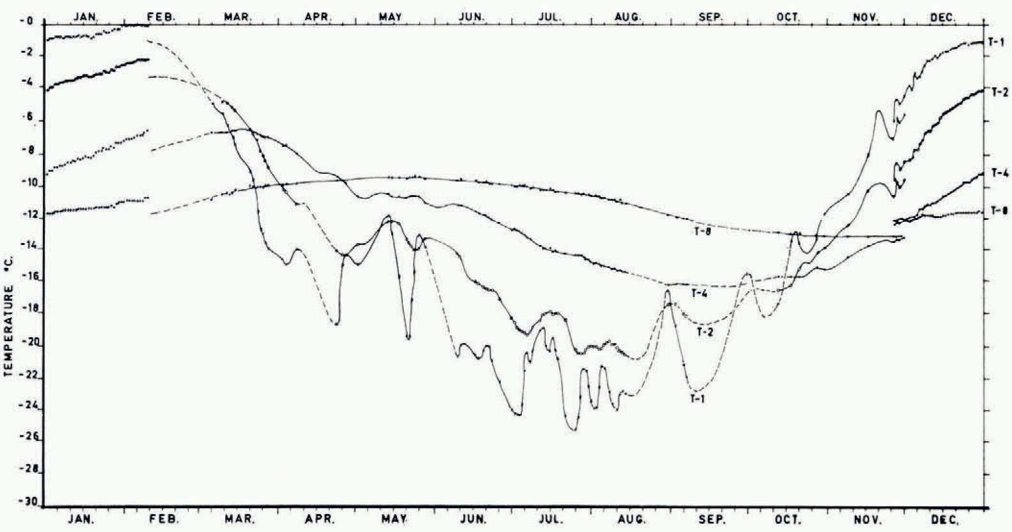

Fig. 1. Daily midnight ice temperatures in the plateau ice at Mawson at depths of 1, 2, 4, and 8 m.

https://doi.org/10.3189/S0022143000020165 Published online by Cambridge University Press

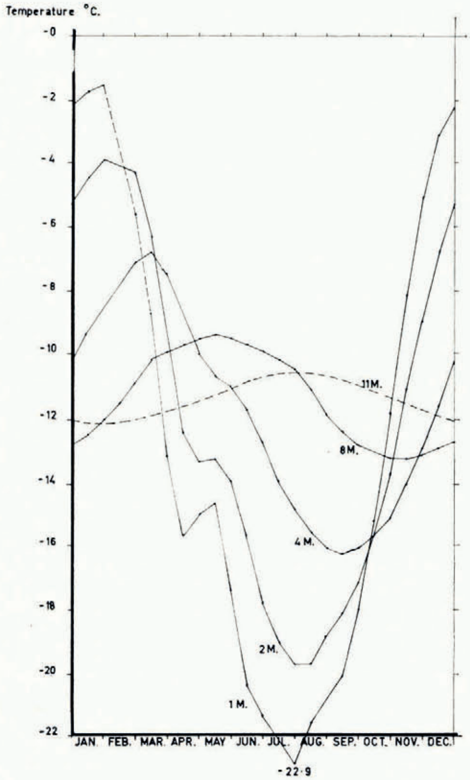

Fig. 2. Half-monthly running means of daily midnight ice temperatures at Mawson at various depths

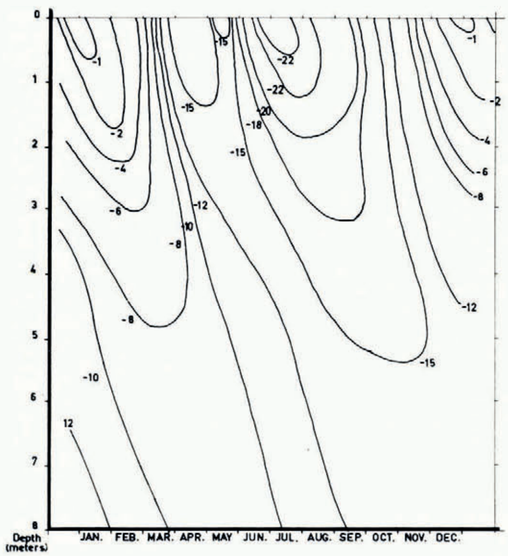

Fig. 3. Temperature isopleths at Mawson. Temperatures are marked in °C.

https://doi.org/10.3189/S0022143000020165 Published online by Cambridge University Press

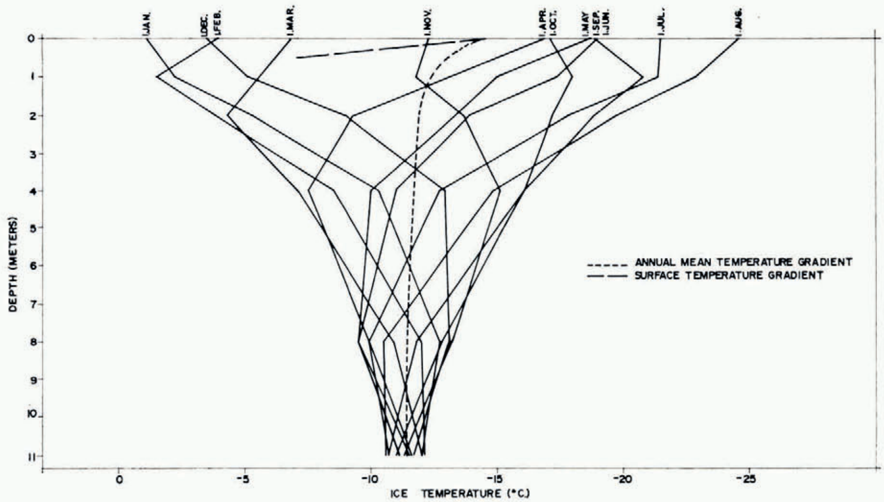

Fig. 4. Temperature profiles in the plateau ice at Mawson at monthly intervals

3. Fourier Analysis of the Plateau Ice Temperatures

It is possible to express the temporal variation of ice temperature at any depth by the Fourier series

$$T = T_{\mathrm{m}} + t\dot{T}_{\mathrm{m}} + \sum_{n} a_n \cos(n\nu t - \alpha_n) \qquad n = 1, 2, 3 \ldots \tag{3.1}$$

where ν is the frequency, n the order of harmonic, a the amplitude, α the phase angle, and T_{m} the mean temperature.

Fourier coefficients for the first twelve harmonics were calculated from the half-monthly running means of temperatures at 1, 2, 4 and 8 m. depth using an IBM 7044 computer. The coefficients for the first three harmonics are shown in Table I.

Table I. Fourier Coefficients for the Annual Ice Temperature Wave at Mawson

z m.	T_{m} °C.	a_1 deg.	a_2 deg.	a_3 deg.	α_1 rad.	α_2 rad.	α_3 rad.
1	−12·48	10·34	1·50	0·48	2·70	3·14	0·71
2	−11·92	7·69	0·71	0·48	2·43	2·69	0·08
4	−11·78	4·30	0·16	0·37	1·78	2·27	−1·17
8	−11·37	1·94	0·10	0·18	0·60	−2·49	−1·98

It is interesting to observe the decrease of the annual mean temperature towards the surface. Budd (in press) has solved the diffusion equation containing radiation as an additional heat-flux term in the ice to explain this change of temperature with depth and has used the above results to verify his solution. The annual mean temperature profile can be explained satisfactorily in terms of absorbed radiation.

4. Thermal Diffusivity of the Ice

A method of ice temperature analysis was selected which is the same as that used by Dalrymple and others (1963) for snow temperature data from the South Pole station and is based on the model by Lettau (1954) for an inhomogeneous body. The two fundamental equations on which it is based are the equation of heat conduction

$$B = -kT' \tag{4.1}$$

and the equation of heat continuity

$$B' = -C\dot{T} \tag{4.2}$$

where B is the vertical heat flux, k the heat conductivity at depth z, C the heat capacity per unit volume at depth z, and T the ice temperature. The prime ($'$) denotes partial differentiation with respect to z; ($\dot{}$) denotes partial differentiation with respect to time t.

From the Fourier series of the ice temperature given in Equation (3.1) it is assumed that the dependent variable B follows from a Fourier series similar to that of T, i.e. that

$$B = B_m + tB_{\dot{m}} + \sum_n b_n \cos(n\nu t - \beta_n) \qquad n = 1, 2, 3, \ldots \tag{4.3}$$

By differentiation with respect to z of both (3.1) and (4.3) and introducing

$$\gamma_n = \alpha_n - \beta_n \tag{4.4}$$

i.e. the phase difference between T' and T waves where

$$\tan \gamma_n = -\frac{\alpha'_n}{(\ln A)'_n}, \tag{4.5}$$

it can be shown (Lettau, 1954) that the thermal diffusivity

$$\bar{K} = \frac{\bar{k}}{\bar{C}} = \frac{n\nu \sin 2\gamma_n}{2\alpha'_n \beta'_n} \tag{4.6}$$

The bar ($^-$) indicates that the values are independent of time.

Equation (4.6) gives a solution for $\bar{K}$, where $\bar{K}$ can vary in any manner with depth. It is thus suitable for inhomogeneous media. The same value of $\bar{K}$ should be obtained for each harmonic n, Lettau has however found that in soil the higher harmonics give different results.

Figure 5 shows coefficients α, β and $\ln A$ of the first harmonic as a function of depth z. Smoothed curves are drawn through the calculated points and α', β' and $(\ln A)'$ are obtained by drawing tangents to the curves at the points required.

The values of the thermal diffusivity obtained using Equation (4.6) are shown in Table II.

The amplitude of subsequent harmonics is too small compared with errors in ice temperature measurements to give significant results. The results of the analysis of the first harmonic

Table II. Fourier Coefficients and Diffusivity from the First Harmonic of Ice Temperatures

z m.	$\ln A$	$-(\ln A)'$	α rad.	α' rad. m.$^{-1}$	γ deg.	β rad.	β' rad. m.$^{-1}$	K cm.^{2} sec.$^{-1}$
1	2·34	0·36	2·70	0·30	39·8	2·00	0·42	0·0078
2	2·04	0·30	2·43	0·30	45·0	1·64	0·40	0·0083
4	1·46	0·23	1·78	0·30	52·5	0·86	0·35	0·0092
8	0·66	0·16	0·60	0·30	57·7	−0·41	0·28	0·0107

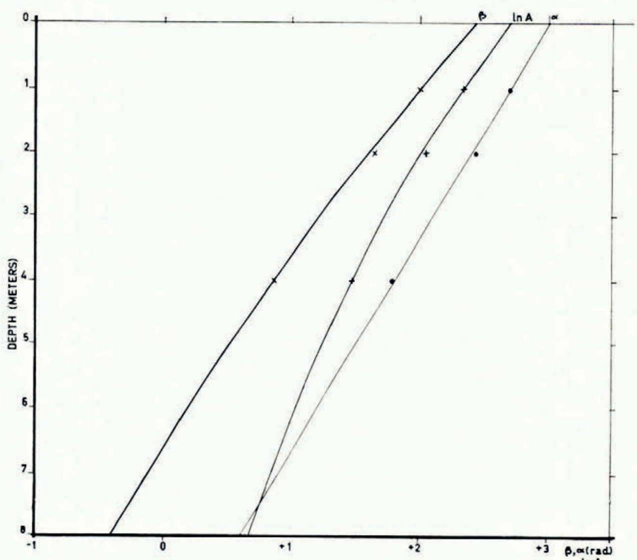

Fig. 5. Coefficients of the first harmonic in the Fourier analysis of temperatures and heat flux at Mawson

https://doi.org/10.3189/S0022143000020165 Published online by Cambridge University Press

however show the interesting fact that the thermal diffusivity decreases as the ice–air interface is approached. Since density measurements of the ice show no variation in the upper metres a genuine change in thermal diffusivity of ice seems unlikely. The apparent change in thermal diffusivity must result from shortcomings of the model used, particularly the assumption that there are no energy sinks or sources within the ice. Ice is in fact quite transparent to short-wave visible radiation (Weller and Schwerdtfeger, in press) and the distribution of the absorbed radiation follows an exponential extinction law from the surface. The least affected value of the thermal diffusivity should be at the 8 m. level where the available energy due to absorbed radiation is negligible. Calculating the thermal conductivity from the diffusivity value at 8 m. depth using the measured ice density ρ of 0·88 g. cm.$^{-3}$ and specific heat capacity 0·48 cal. g.$^{-1}$ deg.$^{-1}$, the conductivity is

$$k = K\rho c = 4\cdot 5\times 10^{-3} \text{ cal. sec.}^{-1} \text{ cm.}^{-1} \text{ deg.}^{-1}.$$

This value compares favourably with values measured elsewhere and the theoretical value of $4\cdot 85\times 10^{-3}$ cal. sec.$^{-1}$ cm.$^{-1}$ deg.$^{-1}$ derived by Schwerdtfeger (1963).

To explain in greater detail the change of diffusivity with depth, the values of diffusivity calculated from phase and amplitude changes of the annual temperature wave will be given now (Table III). They are computed for the first harmonic from Equations (1.4) and (1.3) respectively, taking the data from Table II.

Table III. Thermal Diffusivity of Plateau Ice

Depth m.	*Method of calculation*	*Diffusivity* cm.^{2} sec.$^{-1}$
1	Amplitude change with depth	0·0077
2	Amplitude change with depth	0·0111
4	Amplitude change with depth	0·0188
8	Amplitude change with depth	0·0390
1	Phase change with depth	0·0111
2	Phase change with depth	0·0111
4	Phase change with depth	0·0111
8	Phase change with depth	0·0111

Thus the radiation effect on the phase change with depth is zero in contrast to a large effect on the amplitude. The absorbed radiation reaches the lower depths as a heat flux only, causing a smaller decrease of the amplitude with depth than expected and corresponding increases in K as seen above (Table III). Since only night values of temperature are considered in the initial data the direct effect of radiation is zero. If direct radiation effects (due to imperfect reflectivity of thermocouples) had to be considered then in the upper layers in the ice the direct radiation would give increased amplitudes. In the lower layers amplitude changes would be zero so that one should expect higher K values towards the surface.

The effect of direct radiation thus gives rise to an apparent diffusivity decrease with depth and the effect of heat flux resulting from absorbed radiation gives rise to an apparent diffusivity increase with depth. If radiation is present in ice temperature data which was obtained using non-reflecting thermal sensors then these data may give fairly uniform diffusivity values with depth but these values will be too high.

Considering phase changes now: since there is no phase change with depth of the radiation flux (which is in phase with the temperature at the surface) it will be in phase with the heat flux at some particular depth after one eighth of a period or 6·5 weeks for an annual wave. Since the velocity of propagation into the ice is given by classical theory as $(2K\omega)^{\frac{1}{2}}$ it can be calculated that annual temperature waves penetrate 2·6 m. into the ice in 6·5 weeks. An interesting independent check on this is obtained from Figure 3 which gives approximately 2·5 m. and could thus be used for another diffusivity determination.

At this depth then heat and radiation fluxes are in phase and the phase difference between temperature and heat-flux waves should be 45 deg. From Table II $\gamma = 45$ deg. indeed at 2 m. depth. The increasing values of γ below 2 m. depth are due to increasing phase difference between the heat and radiation fluxes.

A graphical analysis of the phase and amplitude relationship of radiation and heat flux is given later for sea ice.

5. Heat-flux Measurements by Flux Plates

The introduction of heat-flux plates or similar devices into snow or ice for the purpose of heat-flux measurements results in a number of difficulties. First the plates cannot be made perfectly reflecting so that radiation errors in transparent media must be expected and all day readings must be radiation-corrected. The most severe limitation of the flux plate however lies in the fact that unless it is perfectly matched in conductivity to the surrounding medium, the temperature regime in its vicinity will be disturbed, which results in different amounts of heat passing through unit cross-section per unit time for flux plate and medium.

Simple analogue experiments using electrically conducting paper across which different potentials could be applied showed these errors well and will be described elsewhere (Schwerdtfeger, unpublished). They basically showed that the flux through a plate is smaller if its conductivity is less than that of the surrounding medium and vice versa. The heat-flux distortion is controlled by the ratio of the conductivities of flux plate and medium and the thickness to diameter ratio of the flux plates.

Heat-flux plates were installed in vertical bore holes at depths of 1, 2 and 4 m. in the plateau ice. These flux plates (Schwerdtfeger and Weller, 1967) were essentially highly sensitive thermopile ribbon instruments with approximately 600 pairs of thermo-junctions each. The elements were 14 mm. thick and 38 mm. in diameter and were enclosed in a perspex ring 14 mm. thick and 76 mm. in diameter. The bore holes were filled with snow and refrozen with melt water.

To determine the distortion errors of the set of flux plates used in plateau ice and sea ice their output e.m.f. was compared with that expected from temperature gradient measurements in the ice at the same time. About 100 values were analysed as shown in Figure 6. Only night values were used to avoid radiation errors. The scatter is high due to inaccuracies in the graphical method of determining the temperature gradient at a point. The grouped means however show the flux-plate errors for both types of ice. The fact that for a given temperature gradient the flux-plate temperature gradient, given as an e.m.f. reading, is higher than that of the surrounding, means that less flux is passing through the plate than through the surrounding ice.

In the case of sea ice with a thermal conductivity of $4 \cdot 3 \times 10^{-3}$ cal. cm.$^{-1}$ deg.$^{-1}$ sec.$^{-1}$ at the flux-plate depth, compared with plateau ice of conductivity $5 \cdot 3 \times 10^{-3}$ cal. cm.$^{-1}$ deg.$^{-1}$ sec.$^{-1}$ the heat-flux distortion is considerably larger instead of being smaller. This initially somewhat unexpected result is undoubtedly due to heat-flux focussing by the wide perspex ring surrounding the flux-plate element. Correction factors which have to be applied to determine the temperature gradient in the undisturbed ice from flux-plate readings are 0·75 for plateau ice and 0·60 for sea ice. Table IV gives conversion figures to obtain the heat flux in both types of ice.

Table IV. Conversion Table to obtain Ice Heat Fluxes

Measured flux plate e.m.f. mV.	*Sea ice heat flux* $\times 10^4$ cal. cm.$^{-2}$ sec.$^{-1}$	*Plateau ice heat flux* $\times 10^4$ cal. cm.$^{-2}$ sec.$^{-1}$
1	1·30	1·67
2	2·60	3·34
3	3·90	5·00
4	5·20	6·67
5	6·50	8·34
6	7·80	10·00
7	9·10	11·67
8	10·40	13·34
9	11·70	15·00
10	13·00	16·67

https://doi.org/10.3189/S0022143000020165 Published online by Cambridge University Press

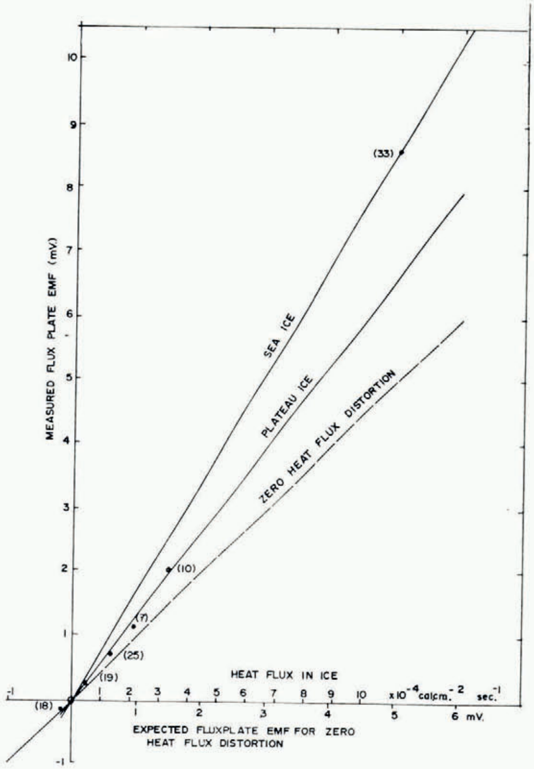

Fig. 6. Heat-flux distortion around a flux plate embedded in ice. The numbers in brackets indicate the number of observations in the plotted group mean

6. Heat-flux Measurements in Plateau Ice

The output of the flux plates measured in millivolts was recorded automatically. Figure 7 shows an example for the variation of heat flux at various depths. Fluctuations of heat flux have been smoothed out considerably by the time the 4 m. level is reached. At that level the heat flux changes sign at the beginning of April from downward to upward flux towards the surface, as the temperature gradient becomes negative due to surface cooling.

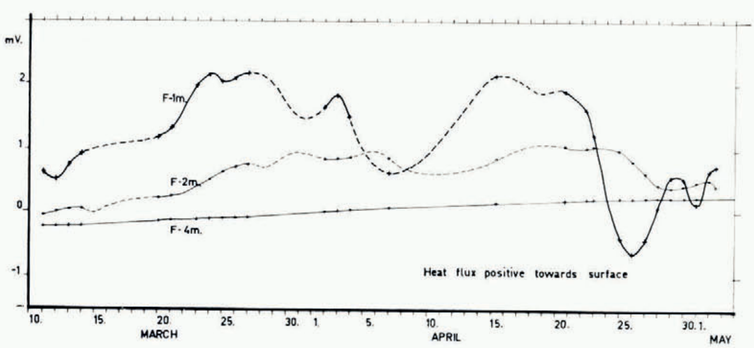

Fig. 7. Heat fluxes at Mawson at 1, 2 and 4 m. depth

https://doi.org/10.3189/S0022143000020165 Published online by Cambridge University Press

The penetration of the temperature waves can again be seen to be preceded by approximately one eighth of a period by the change in heat flux: Figure 7 may be compared with Figure 1; a particular example is presented later (Fig. 9) when the phase and amplitude relationship between heat flux and temperature is used to derive the diffusivity of the ice.

The heat flux can also be determined without the aid of flux plates by considering the rate of change of heat content of the ice. The heat flux through the surface can be computed by determining the total heat gained by the ice by a change of temperature profile with depth $\Delta T(z)$:

$$Q = \rho c \int_0^\infty \Delta T(z)\, dz$$

where ρ the density and c the specific heat of the ice are known. Using the temperature–depth relationship shown in Figure 4 monthly changes in the heat content of the ice can be computed down to 11 m. Changes in heat content below 11 m. are neglected. The results are shown in Table V.

TABLE V. MEAN DAILY ICE SURFACE HEAT FLUX (cal. cm.$^{-2}$ day^{-1})

Jan.	*Feb.*	*Mar.*	*Apr.*	*May*	*Jun.*	*Jul.*	*Aug.*	*Sep.*	*Oct.*	*Nov.*	*Dec.*
+10	+4	−26	−20	−7	−23	−20	−1	+2	+20	+36	+25

+ve sign = heat flux downward −ve sign = heat flux upward

Figure 8 shows the monthly means of the surface temperature and surface heat flux. The phase difference can be numerically determined to be 52 days. The amplitudes of the annual temperature wave A and heat-flux wave B at the surface are approximately 11 deg. and 30 cal. cm.$^{-2}$ day^{-1}. From Equation (1.5) a value of the conductivity is obtained and using $\rho = 0\cdot 88$ g. cm.$^{-3}$ and $c = 0\cdot 48$ cal. g.$^{-1}$ deg.$^{-1}$ the diffusivity can be computed. The values obtained are $k = 0\cdot 0118$ cal. cm.$^{-1}$ deg.$^{-1}$ sec.$^{-1}$ and $K = 0\cdot 028$ cm.^{2} sec.$^{-1}$. These values are more than twice as high as the expected values for ice of density 0·88 g. cm.$^{-3}$. From previous considerations this is not surprising: the heat flux at the surface is not solely due to the surface temperature wave but also due to an additional conducted heat flux due to absorbed radiation. A simple calculation can now show the effect of radiation on the heat flux.

From radiation data at Mawson in 1965 the mean annual amplitude of the short-wave flux directed downward into the ice through the surface is 90 cal. cm.$^{-2}$ day^{-1}. Some of this

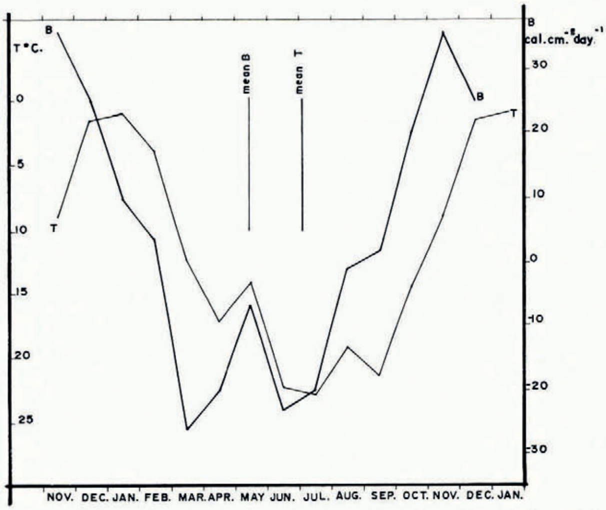

Fig. 8. Monthly means of surface temperature T and surface heat flux B at Mawson

https://doi.org/10.3189/S0022143000020165 Published online by Cambridge University Press

absorbed radiation is stored in the ice, some is lost by conduction to the surface. The radiation effect on the heat storage will be considered first.

Anticipating the results shown below of a diffusivity determination during a radiationless period, namely $K = 0{\cdot}0118$ cm.^{2} sec.$^{-1}$, and using the annual surface temperature amplitude A of 11 deg., from Equation (1.5) an annual amplitude of the heat flux B of only $19{\cdot}5$ cal. cm.$^{-2}$ day^{-1} is computed. Since the measured heat flux has an amplitude of approximately 30 cal. cm.$^{-2}$ day^{-1}, the absorbed radiation must nearly double the heat storage in the ice and the resulting conducted heat flux, giving high amplitudes of B and hence high values of conductivity and diffusivity. The value of A is not affected by absorbed radiation since it is extrapolated from ventilated air temperature sensors.

The heat loss of the ice by conduction due to the presence of an annual mean temperature gradient set up by absorbed radiation will be considered next. This gradient is shown in Table I. The surface temperature was extrapolated by considering the mean of the measured air temperatures at 1 and 4 m. height above the ice for the year to obey a logarithmic profile law and the ice surface temperature to be equal to the air temperature at the height of the mean roughness parameter $z_0 = 0{\cdot}23$ cm.

At the surface of the ice the temperature gradient is 15 deg. m.$^{-1}$, the temperature $-14{\cdot}5$°C. This leads to a heat loss through the surface by conduction of

$$Q = k\frac{\partial T}{\partial z}t = 25{\cdot}0 \text{ kcal. cm.}^{-2}\text{ year}^{-1}$$

or approximately 69 cal. cm.$^{-2}$ day^{-1}. This figure should be compared with the 90 cal. cm.$^{-2}$ day^{-1} of absorbed radiation. For a balanced energy budget of the ice other forms of energy transfer could play a role such as internal melting in the ice, the water vapour reaching the surface of the ice through melted cavities. It seems likely however that the observed difference between heat gain by absorbed radiation and heat loss by conduction is due to the inaccuracy of determining the ice temperature gradient at the surface.

To determine the diffusivity of the ice when there is no radiation present, an isolated sinusoidal temperature pulse and resulting heat-flux wave were taken from the recorded data at 1 m. depth in the plateau ice. The period of the temperature and flux pulses was 7 days, masking any diurnal radiation pattern. Moreover the data were taken from the August records when the incoming radiation is still very low. Flux and temperature pulses are shown in Figure 9.

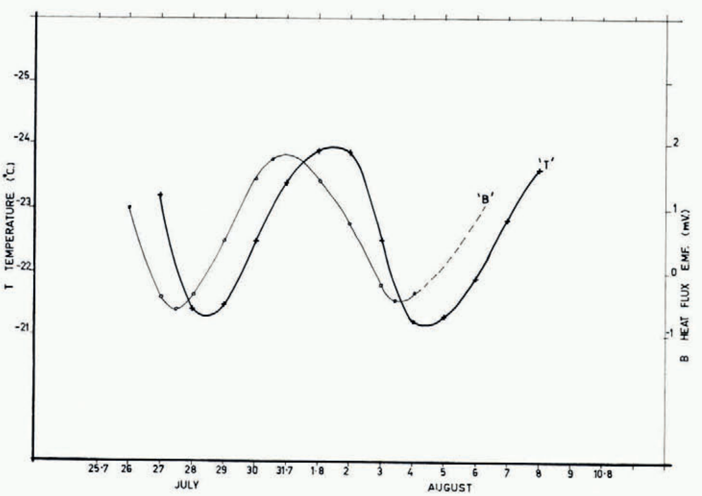

Fig. 9. Waves of heat flux B and temperature T at a depth of 1 m. A selected example

https://doi.org/10.3189/S0022143000020165 Published online by Cambridge University Press

The phase difference between temperature and heat-flux waves is approximately one eighth of a period as expected. Amplitudes are 1·4 deg. and 1·3 mV. respectively, the latter figure is converted by means of Table IV to $2 \cdot 15 \times 10^{-4}$ cal. cm.$^{-2}$ sec.$^{-1}$. From these amplitudes the conductivity and diffusivity can be calculated again using Equation (1.5) and are $k = 5 \cdot 3 \times 10^{-3}$ cal. cm.$^{-1}$ deg.$^{-1}$ sec.$^{-1}$ and $K = 0 \cdot 0118$ cm.^{2} sec.$^{-1}$.

They agree very well with accepted figures for ice and show again that radiation effects must be eliminated when the diffusivity of transparent media is to be computed.

7. Summary of Diffusivity Determinations in Plateau Ice

The results of all plateau ice diffusivity determinations are summarized in Table VI.

Table VI. Summary of Plateau Ice Diffusivity Determinations

Depth m.	*Method of computation*	*Period of waves*	*Diffusivity* cm.^{2} sec.$^{-1}$	*Remarks*
0	Amplitude of T and B	1 year	0·0247	High due to large amount of heat transmitted by radiation
1	Amplitude and phase of T (Lettau's method)	1 year	0·0078	Not a true variation of K with depth, but caused by the effect of radiation penetration on the amplitude–depth profile
2	Amplitude and phase of T (Lettau's method)	1 year	0·0083	
4	Amplitude and phase of T (Lettau's method)	1 year	0·0092	
8	Amplitude and phase of T (Lettau's method)	1 year	0·0107	
1	Amplitude of T	1 year	0·0077	Not true values due to the penetration of radiation. The value at 2 m. is close to the true value since radiation and conduction are approximately in phase here
2	Amplitude of T	1 year	0·0111	
4	Amplitude of T	1 year	0·0188	
8	Amplitude of T	1 year	0·0390	
1	Phase of T	1 year	0·0111	Close to true value because the radiation only has slight effect on variation of phase with depth >1 m.
2	Phase of T	1 year	0·0111	
4	Phase of T	1 year	0·0111	
8	Phase of T	1 year	0·0111	
1	Amplitude of T and B	7 days	0·0118	Close to true value because only conductive heat transfer present (no radiation)

8. Temperature Pattern in Sea Ice—Descriptive Analysis

In the sea ice, as well as in the plateau ice, the temperatures were measured by thermocouples frozen into the ice at 0, 15, 30, 45, 60, 80 and 100 cm. depth. All readings were taken at midnight to reduce radiation errors. A thermocouple at 2 m. depth was always in the sea-water since the maximum ice thickness reached near the thermocouple probe was only 135 cm. Figure 10 shows half-monthly means for all levels. Curves for all levels were extrapolated to $-1 \cdot 8$°C., the freezing temperature of 33‰ salinity sea-water, at the date at which freezing began at that level. Two warm temperature periods, one in early July, the other in late August can be traced throughout the sea-ice cover. In November sea-ice temperature measurements were discontinued; the ice became unsafe to walk on and broke out late in December.

Figure 11 shows tautochrones of sea-ice temperature against depth for half-monthly intervals. Temperature gradients in the early periods of winter are steep and decrease slowly towards the summer months when the greater amounts of absorbed radiation again cause deviation from a linear temperature gradient in the top layer.

9. Heat-flux Measurements in Sea Ice

Heat-flux plates were installed in the sea ice at depths of 30 and 60 cm. Sea-water was allowed to refreeze the bore holes which had been filled with sea ice shavings after installation

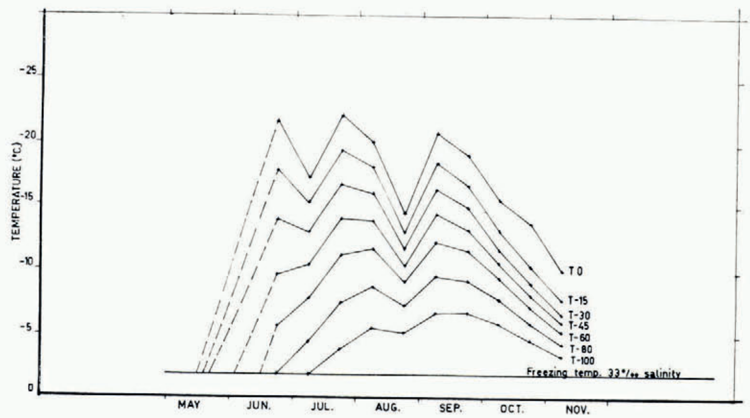

Fig. 10. Half-monthly means of daily midnight sea-ice temperatures at Mawson at various depths marked in cm.

of the flux plates. The flux plate at 60 cm. depth gave inconsistent readings shortly after installation, presumably the plate was not hermetically sealed and electrolytic e.m.f.'s were set up. The flux plate at 30 cm. depth performed well throughout.

One important consequence of heat flux through the sea-ice cover is its effect on the ice growth rate at the ice–water interface. This is shown in Figure 12 where the heat flux at 30 cm. depth is plotted together with the ice growth rate on the same time scale. The phase and amplitude relationship between heat flux and rate of ice growth is obvious. The phase difference is approximately 4 to 5 days depending on the frequency of the heat-flux wave, with the heat flux leading the waves of rate of ice growth. Schwerdtfeger (1966) has used similar data to derive a lag coefficient for sea ice which is of interest in ice growth forecasts. The lag coefficient is inversely proportional to the thermal diffusivity, the proportionality

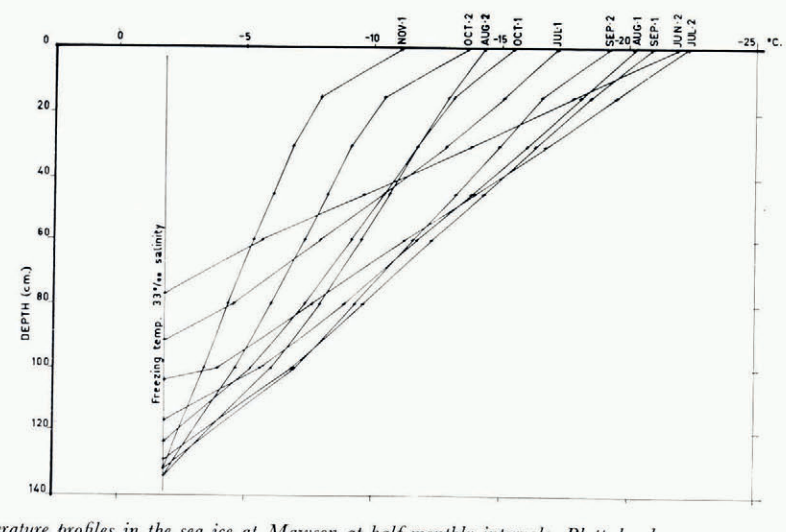

Fig. 11. Temperature profiles in the sea ice at Mawson at half-monthly intervals. Plotted values are means of daily midnight values for the half month

https://doi.org/10.3189/S0022143000020165 Published online by Cambridge University Press

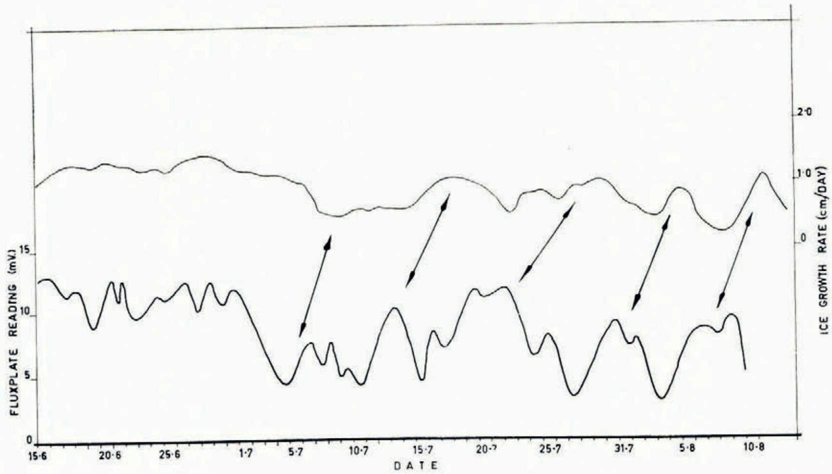

Fig. 12. Heat flux at 30 cm. depth in sea ice and ice growth rate at the ice–water interface. Arrows indicate corresponding peaks

constant being derived empirically. For the above data the constant derived was identical with Schwerdtfeger's.

Sea-ice thickness measurements were carried out fully automatically every six hours through a series of operations where an electric current was passed through a wire loop through the sea ice to heat it, a weight attached to the wire was wound up by an electric motor to the underside of the sea ice and the number of turns of the motor counted and printed. The design of the machine is due to Schwerdtfeger.

With the aid of the flux plates some of the more detailed aspects of heat flux in sea ice such as the diurnal heat flux could be investigated. Figure 13 shows the diurnal variation in heat flux for October. The amplitude of the diurnal variation is remarkable, a change in sign of heat flux occurring quite frequently. It will have to be examined now whether this is a genuine heat flux or whether other effects such as radiation contribute.

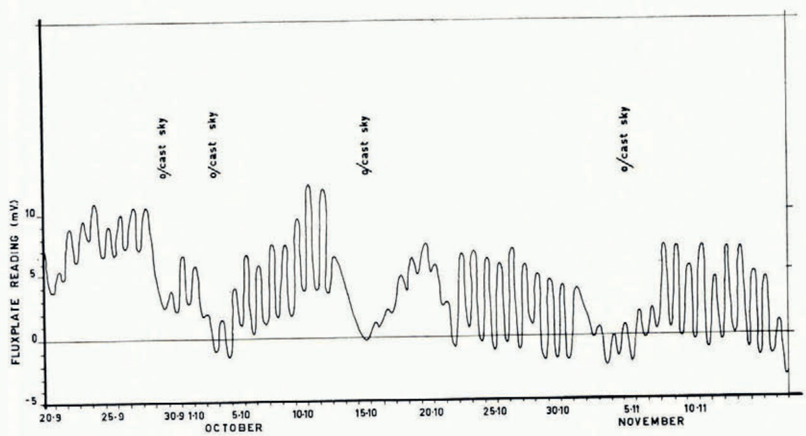

Fig. 13. Diurnal variation of the heat flux at 30 cm. depth in sea ice

10. Thermal Diffusivity of Sea Ice

Figure 14 shows the diurnal variation of heat flux and temperature at the 30 cm. depth in sea ice. The curves are based on mean values for the month of October calculated for hourly intervals. It is apparent that the temperature curve is not a sine wave: the time difference between minimum and maximum temperature is only 9 instead of 12 hours and there is a hump in the curve at approximately 19 hours. The heat-flux curve also shows some deviation from the expected sine-wave shape.

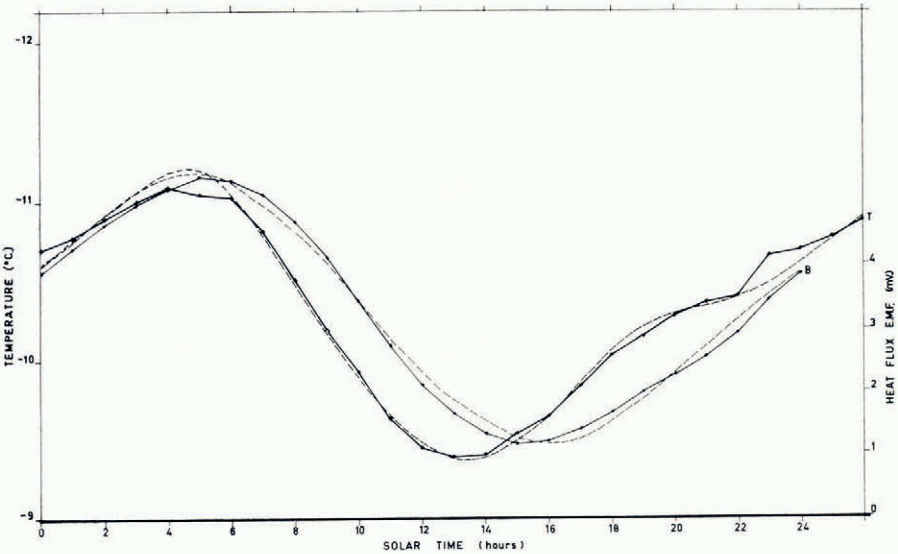

Fig. 14. Heat flux and temperature at 30 cm. depth in sea ice; monthly means for October. The dashed lines are curves derived by a trial-and-error method

If the distortion of the curves is ascribed to radiation penetrating into the sea ice then by superimposing a diurnal radiation pattern on assumed perfect sinusoidal temperature and heat-flux waves one should be able to separate the relative amplitudes and phases of these latter by a trial-and-error method by changing the phases and amplitudes of radiation, temperature and heat-flux waves until the results actually measured are obtained.

The shape of the radiation curve for October has been obtained from Weller (unpublished). Its phase is fixed in relation to solar noon. Using a trial-and-error method to change its amplitude and the phase and amplitude of an assumed sinusoidal temperature wave, a curve can be obtained by addition of the two components (Fig. 15) which closely resembles the mean temperature curve in Figure 14. The immensely strong effect of radiation both on the phase and amplitude of the temperature curve is immediately apparent.

Similarly the heat-flux curve can be obtained (Fig. 16). The effect of radiation on the heat-flux measurements is less severe, since the heat-flux plates are only affected by the net (downward minus upward) radiation at any level in contrast to the thermocouples which are affected by the total (upward plus downward) radiation.

It should be pointed out that the "radiation" curve in both cases indicates the amplitude of the total radiation effect, i.e. the effect of direct radiation on the imperfectly reflecting thermocouples and flux plates as well as the effect of absorbed radiation on the temperature rise and heat flux at 30 cm. depth. Strictly there is a slight phase shift between the direct radiation effect and the temperature rise and heat flux at 30 cm. depth resulting from radia-

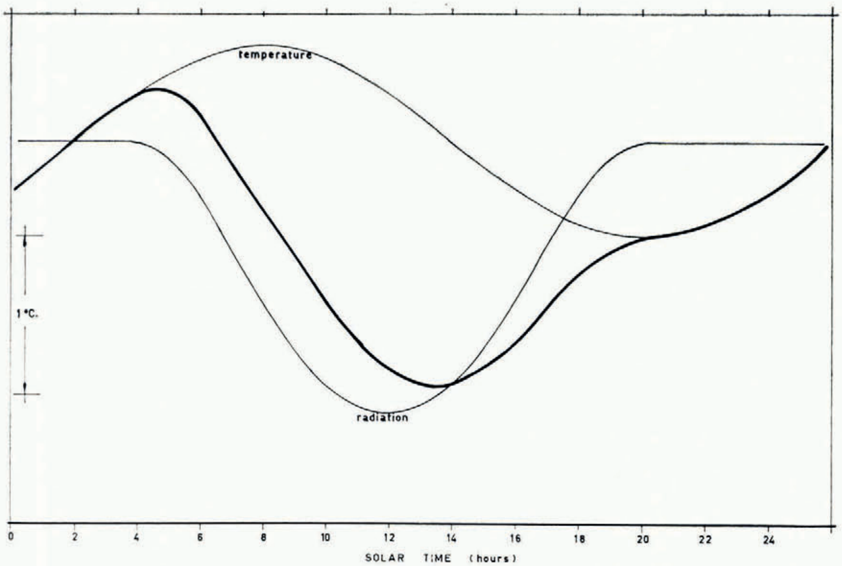

Fig. 15. Trial-and-error determination of the effect of radiation on the diurnal temperature curve at 30 cm. depth

tion absorption in the top 30 cm. For $K = 0{\cdot}01$ cm.^{2} sec.$^{-1}$ the depth of penetration is 15 cm. in one hour for an amplitude reduction of 1/100. Also the direct radiation effect is large in the top layers compared with the heat-flux effect due to absorbed radiation. The small phase shifts involved are therefore ignored.

Drawing the radiation-corrected waves of temperature and heat flux together now (Fig. 17) there appears the correct phase relationship between heat flux and temperature with the heat flux leading the temperature wave by one eighth of a period.

From the amplitudes obtained, namely $0{\cdot}6$ deg. and $2{\cdot}60\times10^{-4}$ cal. cm.$^{-2}$ sec.$^{-1}$ (the peaks of heat flux are $7{\cdot}1\times10^{-4}$ and $1{\cdot}9\times10^{-4}$ cal. cm.$^{-2}$ sec.$^{-1}$), the thermal conductivity can now be derived. Some uncertainty is introduced when values of the density and specific heat must be chosen, neither of which were measured. From Schwerdtfeger (1963) the specific

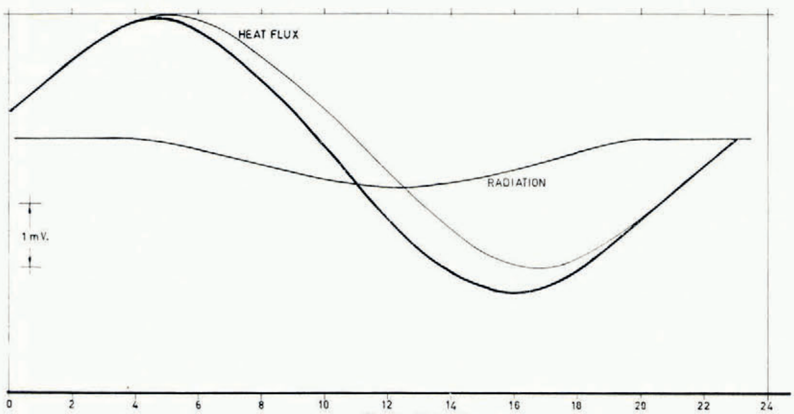

Fig. 16. Trial-and-error determination of the effect of radiation on the diurnal heat-flux curve at 30 cm. depth

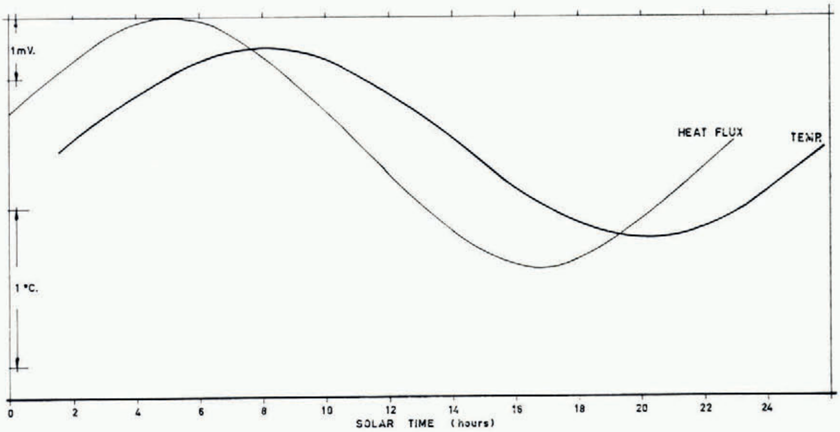

Fig. 17. Radiation-corrected curves of diurnal temperature and heat flux at 30 cm. depth in sea ice at Mawson in October 1965

heat of sea ice of density 0·9 g. cm.$^{-3}$, salinity 6‰ and temperature −12°C. (these latter two values are average conditions measured for October for the top 30 cm. of sea ice) is 0·67 cal. g.$^{-1}$ deg.$^{-1}$. Again $k = (B/A)^2/\omega\rho c$ from Equation (1.5), from which $k = 4 \cdot 30 \times 10^{-3}$ cal. cm.$^{-1}$ deg.$^{-1}$ sec.$^{-1}$ and the diffusivity $K = 0 \cdot 0072$ cm.^{2} sec.$^{-1}$. (The classical solution for semi-infinite thickness can be used here since the depth of penetration for $K = 0 \cdot 007$ cm.^{2} sec.$^{-1}$ is 65 cm. for an amplitude reduction of 1/100 and the sea-ice thickness is 135 cm.) The value of conductivity given by Schwerdtfeger for ice of the same specification is $4 \cdot 69 \times 10^{-3}$ cal. cm.$^{-1}$ deg.$^{-1}$ sec.$^{-1}$ or $K = 0 \cdot 0078$ cm.^{2} sec.$^{-1}$.

Despite uncertainties in the values assumed for ρ and c the value obtained for the thermal conductivity is close to the expected value. Radiation effects seem therefore to have been successfully eliminated and the above curves (Figs. 15–17) are essentially correct.

The fluctuations of heat flux shown in Figure 13 are then basically quite realistic, although the amplitudes should be reduced slightly. They demonstrate the powerful effect of the diurnal surface temperature pattern on the sea ice and the direct contribution of solar radiation to its final summer melting and break-up.

11. Diffusivity Profile in Sea Ice

An attempt will now be made to determine the change of thermal diffusivity with depth in sea ice. As has been shown above only data collected during a radiationless period can be used for this purpose. From the half-monthly sea-ice temperatures a 50-day period warm wave through the sea ice was obtained (Fig. 18). This wave occurred in August when radiation

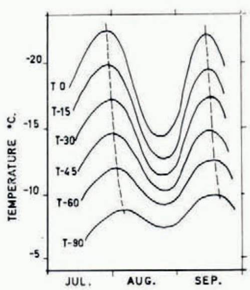

Fig. 18. Amplitude and phase changes of a 50-day period warm wave travelling through the sea ice at Mawson; depths are indicated in cm.

https://doi.org/10.3189/S0022143000020165 Published online by Cambridge University Press

effects are still quite small and can be neglected. (The average value of daily insolation in August is 30 cal. cm.$^{-2}$ day^{-1} compared with 750 cal. cm.$^{-2}$ day^{-1} in December; also during August there is 4–5 cm. constant snow cover on the sea ice.)

Small changes of sea-ice thickness due to ice growth were neglected and an average thickness of 125 cm. was taken. Salinity profiles were measured and are shown in Table VII together with the average ice temperature at that level for the duration of the wave. From these data and using Schwerdtfeger's (1963) theoretical considerations, values of diffusivity could be derived for various levels.

Table VII. Variation of Properties of Sea Ice with Depth

Depth cm.	*Salinity* ‰	*Temperature* °C.	*Diffusivity* cm.^{2} sec.$^{-1}$
0	7	−18	0·0098
30	6	−14	0·0093
60	5	−11	0·0083
100	4	−6	0·0052
125	4	−2	0·0010

To analyse the wave data, the solution given by Carslaw and Jaeger (1959) for a slab with periodic surface temperature was used. A slab $0 < x < l$ with zero initial temperature and with the planes $x = 0$ and $x = l$ kept at zero and $\sin(\omega t + \epsilon)$ respectively is considered. The solution for temperature is of the form

$$A = \left\{\frac{\cosh 2hx - \cos 2hx}{\cosh 2hl - \cos 2hl}\right\}^{\frac{1}{2}} \tag{11.1}$$

and

$$\phi = \arg\left\{\frac{\sinh hx(1+i)}{\sinh hl(1+i)}\right\} \tag{11.2}$$

where A is the amplitude, ϕ the phase, and $h = (\omega/2K)^{\frac{1}{2}}$ where K is the diffusivity. Amplitudes are obtained from Figure 18 and are given in Table VIII.

Table VIII. Amplitude of Temperature Wave in Sea Ice

Depth cm.	*Amplitude* deg.	*Relative amplitude* A	*Relative depth* x/l
0	4·0	1·00	0
15	3·5	0·87	0·12
30	2·9	0·73	0·24
45	2·4	0·60	0·36
60	1·9	0·47	0·48
80	1·2	0·30	0·64

Solutions of Equation (11.1) for various diffusivities K are easily obtained graphically using the above data and a series of values of hl and hx. This is shown in Figure 19 where the dotted line represents the actual sea-ice amplitude data. Interpolating between the values of hl or K, the diffusivity can be obtained for various depths such as shown in Table IX.

Table IX. Diffusivity of Sea Ice Deduced from Temperature Wave

Relative depth	hl	*Diffusivity* K cm.^{2} sec.$^{-1}$	*Depth* cm.
0·1	1·10	0·0094	12·5
0·2	1·12	0·0091	25
0·4	1·26	0·0072	50
0·6	1·62	0·0043	75
0·8	1·81	0·0035	100
0·9	2·00	0·0029	112·5

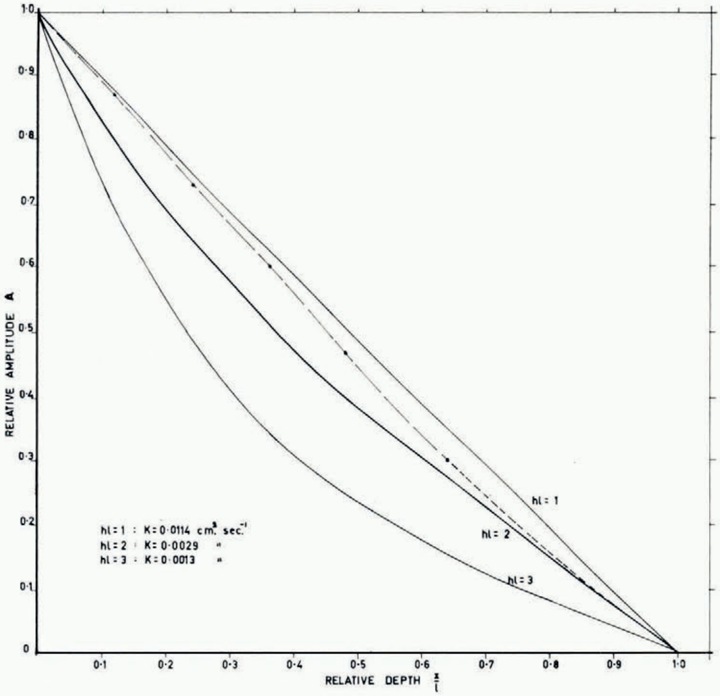

Fig. 19. Amplitude decrease of a 50-day period wave in sea ice at Mawson (dashed line) compared with theoretical solutions for a slab with fixed bottom temperature and a harmonic wave at the surface for various values of the diffusivity K and the corresponding parameter hl

These values together with the data obtained from theoretical considerations above are shown in Figure 20. The diffusivity decreases with depth as expected and agrees generally with the theoretical values. However, the error bars indicate that temperature is quite critical in the analysis of the amplitude reduction with depth, an error of $\pm 0 \cdot 1$ °C. changing the diffusivity appreciably. The factor that affects the theoretical values most is the salinity, and the error bars in Figure 20 show that a change of ± 1‰ in salinity can also change the diffusivity appreciably, particularly at higher ice temperatures.

A simplification of matters was also introduced by considering a stationary lower boundary. Actually the boundary advanced *c.* 10 cm. due to ice growth in the period considered. This would slightly increase the amplitudes of the temperature wave at the lower levels and hence decrease the diffusivity. Compared with the errors of the above method this change would however appear to be inconsequential. The accuracy of the available data does not permit diffusivity calculations from phase changes.

12. Conclusion

It has been shown that to determine the thermal diffusivity in optically transparent media such as ice, it is necessary to consider the effect of radiation transmitted through the medium. This effect is twofold: first, direct radiation on temperature or flux sensors in the ice results in large errors if these sensors are not perfectly reflecting; secondly, the radiation is absorbed exponentially with depth and a heat flux results which is additional to that due to temperature pulses at the surface.

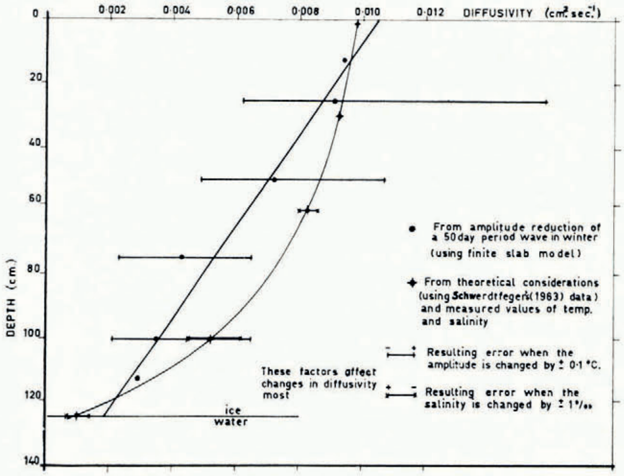

Fig. 20. Diffusivity of sea ice at Mawson determined from the amplitude reduction of a temperature wave and from theoretical considerations

If radiation effects are not separated, diffusivity values obtained may be either too high or too low depending entirely on the method used for computation.

The same considerations apply to snow and other optically translucent media. The consequences of this on heat flux and temperature measurements, particularly in polar regions, are obvious.

ACKNOWLEDGEMENTS

The author is indebted to Dr. P. Schwerdtfeger of the University of Melbourne and Mr. W. Budd of A.N.A.R.E. for help and advice on the field work and data treatment. Thanks are also due to Mr. G. Martin for assistance in the maintenance of the equipment at Mawson and Mr. J. Straede of the University of Melbourne for writing the IBM computer programme for the data reduction. The director of A.N.A.R.E. has given permission to publish this paper.

MS. received 17 February 1967 and in revised form 5 May 1967

REFERENCES

Budd, W. In press. Ablation from an Antarctic ice surface. [Paper read at International Conference on Low Temperature Science, Sapporo, August 1966, to be published.]

Carslaw, H. S., *and* Jaeger, J. C. 1959. *Conduction of heat in solids. Second edition.* Oxford, Clarendon Press.

Dalrymple, P. C., *and others.* 1963. South Pole micrometeorological program. Part II: data analysis by P. C. Dalrymple, H. H. Lettau and S. H. Wollaston. *U.S. Quartermaster Research and Engineering Center, Natick, Mass. Technical Report* ES-7.

Lettau, H. H. 1954. Improved model of thermal diffusion in the soil. *Transactions. American Geophysical Union*, Vol. 35, No. 1, p. 121–32.

Schwerdtfeger, P. 1963. The thermal properties of sea ice. *Journal of Glaciology*, Vol. 4, No. 36, p. 789–807.

Schwerdtfeger, P. 1966. On the response of a sea-ice cover to changes in surface temperature. *Journal of Glaciology*, Vol. 6, No. 45, p. 439–42.

Schwerdtfeger, P. Unpublished. The measurement of heat conduction in the ground. [Presented to A.N.Z.A.A.S. Conference, Melbourne, Australia, January 1967.]

Schwerdtfeger, P., *and* Weller, G. 1967. The measurement of radiative and conductive heat transfer in ice and snow. *Archiv für Meteorologie, Geophysik und Bioklimatologie*, Ser. B, Bd. 15, Ht. 1–2, p. 24–38.

Weller, G. Unpublished. Radiation fluxes over an Antarctic ice surface. [M.Sc. thesis, University of Melbourne, 1964; to be published as an A.N.A.R.E. report.]

Weller, G., *and* Schwerdtfeger, P. In press. Radiation penetration in Antarctic plateau and sea ice. *W.M.O. Technical Note.* [Proceedings of Symposium on Polar Meteorology, Geneva, 1966.]